

## Density Functional Theory calculations on the magnetic properties of the model tyrosine radical–histidine complex mimicking tyrosine radical $Y_D^\bullet$ in Photosystem II

MARCIN BRYNDA\* and R. DAVID BRITT

*Department of Chemistry, University of California Davis,  
One Shields Avenue, Davis, California, 95616, USA*

Received 20 April 2006; accepted 24 May 2006

**Abstract**—Results of Density Functional Theory (DFT) theoretical investigations, which use a model Tyr (Tyr) radical and Tyr–His (Tyr–His) complex to mimic the  $Y_D^\bullet$  radical in Photosystem II (PSII) are presented and compared to experimental results from  $^{15}\text{N}$  Electron-Nuclear Double Resonance spectroscopy (ENDOR) studies of the  $\tau$  nitrogen coupling from His-189 in the PSII Tyr–His complex. The DFT calculations are performed using an optimized geometry of the tyrosine radical and Tyr–His complex. The conformational space of the Tyr–His tandem is explored by varying the relative geometry of the two components; relevant parameters, such as the spin distribution on the phenoxy-ring carbons of the Tyr radical and the EPR hyperfine tensors, are calculated at each geometry and compared with the available experimental data. The isotropic  $^{15}\text{N}$ -ENDOR signal arising from spin delocalization on the His hydrogen-bonded to the PSII tyrosine radical is analyzed in terms of the DFT obtained parameters. The calculations of the  $g$  tensor using the Gauge Independent Atomic Orbital (GIAO) approach are presented and the influence of the geometry of the Tyr–His complex on the deviation of the  $g$ -tensor elements from the free electron values is discussed.

*Keywords:* Photosystem II; DFT; ENDOR; His–tyrosine complex.

### INTRODUCTION

In many biological systems, enzymatic reactions occur in which the tyrosine (Tyr) radical has been described as an important intermediate. One of the most studied systems in which the Tyr radical is observed is Photosystem II (PSII), in which a light driven chain of reactions involves Tyr radicals. PSII contains two redox-active tyrosines,  $Y_D$  and  $Y_Z$ , which are located in the reaction center polypeptides D2 and D1 [1–7]. Although there exists an abundance of experimental data

---

\*To whom correspondence should be addressed. Tel.: (1-530) 754-4141; Fax: (1-530) 752-8995; e-mail: [mabrynda@ucdavis.edu](mailto:mabrynda@ucdavis.edu)

regarding the characteristics of the Tyr radical in various chemical environments, corresponding theoretical computational studies with respect to this important paramagnetic intermediate have been less extensive. Several topics related to the electronic structure of the Tyr radical, as well as its role in electron transfer have been addressed at various levels of theory. In the early 1990s, several attempts to calculate the proton hyperfine couplings were made using semi-empirical methods [8, 9]. The first attempts to use DFT theory focused on the calculations of Tyr radical geometry, the IR frequencies [10], as well as the characteristics of the  $g$ -tensor [11]. Simple models were used to obtain the relevant information about the electronic structures and magnetic properties of the Tyr radical, most importantly including different phenoxy derivatives [12–14].

The influence of the electronic environment on the  $g$ -tensor values have been extensively studied by many groups. The relation between the hydrogen bond to the phenoxy oxygen and the  $g$ -values on the Tyr has been theoretically investigated [15, 16] and recently new computational schemes were proposed for the calculation of the  $g$ -tensor [17, 18]. Moreover, DFT calculations on a Tyr radical dipeptide analogue including a continuum solvent model as well as the explicit water molecules have been also carried out [19]. One of the most addressed topics which is widely covered experimentally is the spin distribution on the Tyr ring. Calculations of the spin distribution as well as  $^{13}\text{C}$  and  $^1\text{H}$  hyperfine couplings on selectively labeled carbons and protons in phenoxy ring were presented in several papers [20–22]. These calculations were also undertaken for the Tyr radical in its radical anion (negative carboxylate ion of the terminal  $\text{COO}^-$  group) form [23].

Specific approaches were developed in order to understand the mechanistic aspects of important reactions in which the Tyr radical is involved with the help of quantum mechanical methods. These include a simple model for Tyr oxidation in phenyl-imidazole complexes [24], formation of the neutral Tyr radical and regeneration of the neutral Yz tyrosine in PSII [25], involvement of the Tyr radical in the reaction mechanism with NADPH, histidine (His) and Tyr [26] and hydrogen abstraction from manganese-coordinated water by a Tyr radical [27]. Finally a number of calculations on the electronic structure and magnetic characteristics of various tyrosine derivatives such as thioether-substituted Tyr radical [28–30] were also conducted.

Despite this broad spectrum of the specific points of interest targeted by theoretical approaches, only few computational studies devoted directly to the Tyr radical (in  $\text{Y}_Z$  or  $\text{Y}_D$  form) in PSII are available. Strikingly, no computational data have been reported for the experimentally-conjectured Tyr-His complex, with the exception of some early computational studies by Un *et al.* [11] (in which the His hydrogen donor was mimicked by the imidazole ring) and a similar DFT study by Wang *et al.* [25]. The available QM results concern different types of radicals with most theoretical studies focused on various phenoxy derivatives. Among the most important issues, the following are of substantial importance: The reported calculations dealing with the Tyr radical were performed on different model molecules

with conformational and magnetic characteristics that are not comparable. Moreover, different calculations were performed in various oxidation states (e.g., neutral *vs.* positively/negatively charged molecules), showing a real interest for these species, but unfortunately leading to a significant amount of non-comparable data. The models used to describe the Tyr radical in PSII vary from simple phenoxy radical, through isolated Tyr radical to peptides homologues of the Tyr. Another factor which complicates the comparison of the theoretical results is the fact that in different calculations the overall spin density on the phenoxy ring varies from 0.8 to 1.2 (the remaining positive or negative spin being delocalized on the imidazole or similar partner), thus making difficult the comparison of the calculated spin distribution on selected ring atoms. Finally, the *g*-tensor calculations were performed on various molecules mimicking the Tyr radical, with the hydrogen bond from the His being modeled in different manners. Having in mind all these issues, we thus decided to carry out a more systematic DFT study on the stable  $Y_D^\bullet$  radical of PSII with an emphasis on comparisons with available experimental data.

## MODEL AND COMPUTATIONAL METHODS

The DFT calculations were performed for three distinctive types of radicals: Neutral ( $R^\bullet$ ), radical cation ( $R^{\bullet+}$ ) and radical anion ( $R^{\bullet-}$ ). Since the Tyrosine radicals of PSII are formed by electron donation to the highly oxidizing  $P680^+$  radical, only oxidized tyrosine states are relevant for PSII function. Neutral radical forms (oxidized and deprotonated) are highly favored given both experimental magnetic resonance data [31] and the calculated  $pK_a$  (approx.  $-3$ ) for a Tyr cation radical [32]. However, it is not inconceivable that under some conditions a cation tyrosine radical form (OH remaining protonated) could be stabilized, and it is therefore useful to consider EPR observables that would provide evidence for such a state. These include *g*-tensor elements and proton/deuteron hyperfine couplings, particularly for the exchangeable hydrogen OH group. Although it has been widely agreed [12] that the Tyr radical is present in its neutral  $Y_D$  form in PSII, we found it useful to extend this computational study to include the radical anion (the radical anion is modeled by a Tyr radical with the deprotonated backbone acetate group in lieu of an extended backbone which is present in the protein; this should not be confused with reduced Tyr radical anion with a formal charge of  $-2$ ), as some of the data reported in the literature arises from experimental and theoretical studies of Tyr radical in this particular form [23]. The data reported and herein will focus primarily on the neutral Tyr radical and the neutral Tyr-His complex; Tyr radical cation and Tyr radical anion will be considered for comparison purposes.

For both  $R^\bullet$  and  $R^{\bullet-}$  forms, the applied methodology was identical. In a preliminary step, the geometry of an isolated, single Tyr radical was optimized. Then, a series of optimizations and subsequent calculations were performed, using the minimum energy structure as a starting point. In the second phase, the geometry of a His molecule was optimized [33] and the His-Tyr complex was reoptimized at

this step. Finally, a His-Tyr complex conformational space was scanned by moving the position of the His molecule (using frozen coordinates) around the fixed Tyr molecule and executing the calculations of the magnetic properties at each different geometry of the Tyr-His complex in order to obtain relevant information about the EPR parameters that are later analyzed in the light of the existing experimental data. For the radical cation form ( $R^{\bullet+}$ ), the geometry of the isolated Tyr radical cation (without the His partner) was optimized.

The following designations are used throughout the text: neutral Tyr radical ( $TR^{\bullet}$ ), Tyr radical anion ( $TR^{\bullet-}$ ), neutral Tyr-His radical ( $THR^{\bullet}$ ), Tyr-His radical anion ( $THR^{\bullet-}$ ), neutral dipeptide analogue of the (Ala-Tyr-Ala)-His radical ( $DPTHR^{\bullet}$ ) and Tyr radical cation ( $TR^{\bullet+}$ ).

For all the calculations of the magnetic properties, the EPR-II basis set of Barone and co-workers in conjunction with a hybrid B3LYP functional as implemented in the Gaussian 03 package [34] was used. This basis set was successfully used for the DFT calculation of the effect of the orientation of the hydrogen bond donation on the hyperfine coupling of benzosemiquinones [35]. The choice of the EPR-II basis set was checked against the use of the larger EPR-III basis set. The resulting calculated trends are not significantly different; however the calculations with EPR-III basis set are considerably more time consuming. The geometries of the isolated Tyr radicals ( $TR^{\bullet}$ ,  $TR^{\bullet-}$ , and  $TR^{\bullet+}$ ), as well as of the neutral dipeptide analogue of the (Ala-Tyr-Ala)-His radical ( $DPTHR^{\bullet}$ ) were optimized at the B3LYP/6-31G\* level; those of Tyrosine-His complexes ( $THR^{\bullet}$  and  $THR^{\bullet-}$ ) were fully optimized at the B3LYP/6-31G\*, B3LYP/6-31+G\* and B3LYP/6-31++G\*\* levels with basis sets incorporating one or two diffuse functions. For the calculation of the  $g$ -tensor, the Gauge Independent Atomic Orbital (GIAO) method [36] as implemented in Gaussian 03 was used. For the sake of consistency, the calculations of the  $g$ -tensor for some selected geometries were repeated using the Amsterdam Density Functional (ADF) program [37]. Specific information about the theoretical level used in each particular set of calculations is reported with the corresponding computational data.

## RESULTS AND DISCUSSION

### *Isolated Tyr radical*

The optimization of the geometry for the isolated Tyr radical results in three distinguishable minima (data not shown) and is in agreement with the previous QM studies [10]. The lowest energy minimum (Fig. 1A) was used as a starting point for a set of calculations in which the orientation of the  $\beta$ -hydrogens *versus* the plane containing the phenoxy ring was successively varied. At each step of this conformational scan, the geometry of the molecule was fully reoptimized. The calculated EPR parameters were used to analyze the McConnell relation for the hyperfine (HF) couplings of Tyr  $\beta$ -hydrogens.

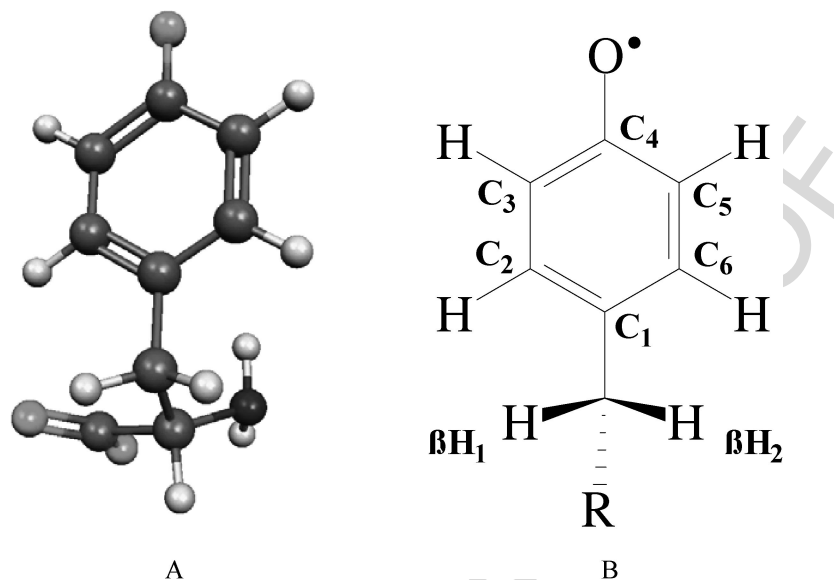


**Figure 1.** (A) DFT optimized structure of the isolated neutral Tyr radical; (B) atom numbering scheme for the Tyr radical.

The hyperfine coupling of the  $\beta$ -hydrogens in the Tyr radical is a relevant conformational parameter which has been extensively studied by experimental techniques [12, 20, 38–41]. From experimentally determined isotropic hyperfine couplings using the simple McConnell relation

$$A_{\text{iso}} = B \cdot \rho C_1 \cdot \cos^2(\theta), \quad (1)$$

where  $B = \text{constant}$ ,  $\rho C_1 = \text{spin density on carbon } C_1$  and  $\theta = \text{angle between normal to the phenoxy ring and } C-\beta\text{H bond direction}$ , one can estimate the orientation of the  $\beta$ -hydrogens *versus* the phenoxy ring. The value of the isotropic part of the hyperfine interaction  $A_{\text{iso}}$  on the  $\beta$  protons is governed by the mutual orientation of the  $C-\beta\text{H}$  bond *versus* the principal axis of the  $p_z$  orbital of the neighboring  $C_1$  carbon atom, which bears a large amount of the unpaired electron spin. From the experimental studies [20, 39, 42] it was suggested that the angles between the two  $\beta$  protons and the phenoxy ring are quite different, depending on the Tyr chemical environment (Table 1). Our DFT calculated values for these angles ( $61.9^\circ$  and  $57.3^\circ$  for the neutral His-Tyr complex and  $60.8^\circ$  and  $58.4^\circ$  for the isolated neutral Tyr radical) correspond to the optimized structures on which no constraints were imposed related to the peptide chain connected to the Tyr moiety. These angles are close to  $60^\circ$ , a situation in which both  $\beta$  hydrogens lie symmetrically on two opposite sides of the plane perpendicular to the phenoxy ring and containing the carbons  $C_1$  and  $C_4$  (Fig. 1B). This is, however, in contrast with the experimentally reported angles for various tyrosines, in which a pronounced asymmetry of the  $\beta\text{H}_1$

**Table 1.**

Selected experimental values of  $\theta$  angles (angle between  $\beta$ -protons and phenoxy ring, see text for details) for the Tyr radicals in PSII in various organisms

Angle		Reference
$\beta\text{H}_1$	$\beta\text{H}_2$	
$47 \pm 2$	$73 \pm 2$	[42]
$75 \pm 15$	$45 \pm 15$	[42]
$52 \pm 4$	$68 \pm 4$	[20]
61.9	57.3	Calc. THR $\bullet$
60.8	58.4	Calc. TR $\bullet$
52.7	66.6	Calc. DPTHR $\bullet$

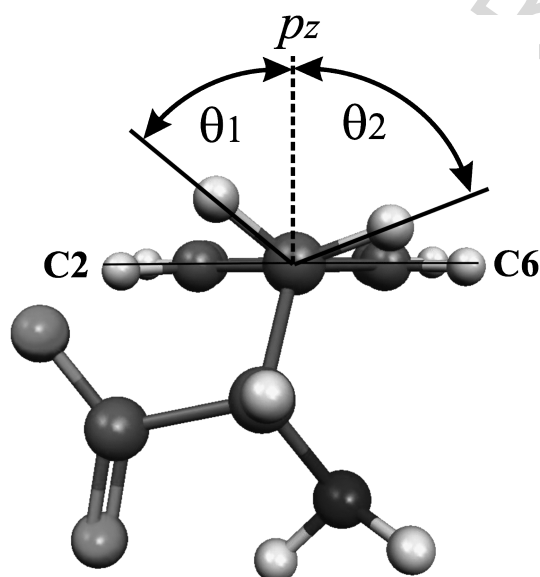


**Figure 2.** Schematic representation of the  $\theta$  angles between  $\beta$ -protons and the plane containing the phenoxy ring of the Tyr radical.

and  $\beta\text{H}_2$  is observed and, therefore, suggests that steric constraints are present in the real biological systems.

We have performed a series of calculations on the Tyr radical model by varying the  $\theta_1$  (and automatically the  $\theta_2$ ) angle (Fig. 2). From the curves of the dependence of the  $\beta$ -protons  $A_{\text{iso}}$  we have determined that in our computational model, the constants appearing in the McConnell equation relating the HF couplings to the orientation of the  $\beta$ -protons are not exactly the same for  $\beta\text{H}_1$  and  $\beta\text{H}_2$ . The analogous observed asymmetry concerning the HF couplings of the phenoxy ring protons was pointed out in the recent DFT study by Langella *et al.* [19] on the dipeptide analogs of Tyr radicals.

In Fig. 3A and 3B are presented the curves of computed  $A_{\text{iso}}$  for the protons  $\beta\text{H}_1$  and  $\beta\text{H}_2$  as a function of  $\theta_1$  ( $\theta_2$ ), the angles between the direction of the principal

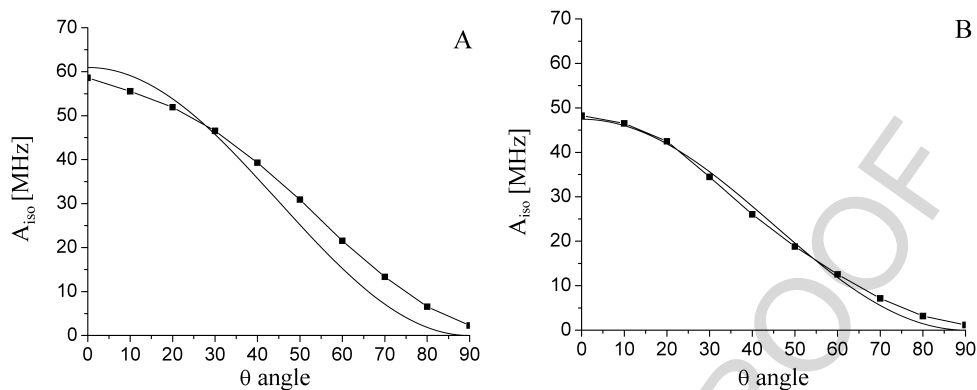


**Figure 3.** Graph of calculated  $A_{\text{iso}}$  values (solid line with squares) for the protons  $\beta\text{H}_1$ (A) and  $\beta\text{H}_2$ (B) as a function of  $\theta_1$  ( $\theta_2$ ); curve fit (smooth grey line).

axis of the  $p_z$  orbital (perpendicular to the plane of the phenoxy ring) of the carbon  $C_1$  and the direction of the  $\beta\text{H}_1\text{-C}$  ( $\beta\text{H}_2\text{-C}$ ) bonds (Fig. 2). The fitting procedure yields two slightly different values for the  $B$  constant in the McConnell relation. It is worth noting that the computed spin density on  $C_1$  is almost unaffected by the changes in the orientation of the  $\beta$ -hydrogens (for the rotation over a 90 degrees range  $\rho_{C_1} = 0.341\text{--}0.345$ ). Thus the ranges of  $B_1$  and  $B_2$  and their mean values were calculated using the upper and lower limits, as well as the average value of the computed spin density on carbon  $C_1$ .

$$A_{\text{iso}}(\beta\text{H}_1) = B_1 \cdot \rho_{C_1} \cdot \cos^2(\theta_1) \quad (2)$$

$$A_{\text{iso}}(\beta\text{H}_2) = B_2 \cdot \rho_{C_1} \cdot \cos^2(\theta_2). \quad (3)$$

The computed mean values of  $B_1$  and  $B_2$  are 49.5 and 55.0 G, respectively, calculated with an average  $\rho_{C_1}$  value of 0.342 ( $B_{\text{av}} = (B_1 + B_2)/2 = 52.3$  G). The upper and lower limits of the  $B_1$  and  $B_2$  values calculated with the maximum and minimum  $\rho_{C_1}$  values are 49.1–49.7 and 54.5–55.1 G, respectively. This result is also in excellent agreement with the DFT calculations of the  $B$  value for fully symmetrical  $\beta$ -protons couplings in *p*-ethylphenoxy radical [12] where  $B$  was reported to be 52.4 G, which corresponds almost exactly to our calculated value of  $B_{\text{av}}$ . Our results may indicate that special care must be taken while estimating the orientation of the  $\beta$ -protons from the experimental data; the revealed asymmetry (at least in the QM calculations) of the hyperfine couplings can be a factor seriously affecting the calculated angles between the  $\beta$ -protons and the phenoxy ring. In this context the value of 58 G [41], suggested in 1963 by Fassenden and Schuler [43], for the  $B$  parameter in the McConnell relation used by the majority of the authors might not only be overestimated, but also inappropriate, as two separate constant should be used for the two slightly non-equivalent  $\beta$ -protons.

In order to check the validity of our calculations and the accuracy of the obtained parameters, we have analyzed the spin distribution and the corresponding isotropic parts of the hyperfine tensors for the phenoxy ring atoms. The calculated spin

distribution, as well as the isotropic Fermi contact values for some protons in the lowest energy conformation for isolated Tyr radical, are reported in Table 2. The computed spin densities are in reasonable agreement with previously calculated and experimentally determined spin densities for various Tyr radicals. Due to the important amount of the experimental values reported for this radical we have performed the analysis of the results of our calculations in two steps. First we have compared our theoretical DFT results with the results available from different quantum mechanical calculations, and in the second step our data were compared with some selected experimental studies.

The calculated isotropic coupling constants are very close to those reported recently by Langella *et al.* [19], in the DFT calculations on the Tyr radical dipeptide analogue at PBE0/EPR-II level (without considering solvent effects). Similarly, the DFT results for the hyperfine couplings calculated in phenoxy and p-methylphenoxy radical at PWP86/IGLO-III level [12] are very close to those reported here.

For the comparison purposes the calculations were also carried out on the radical cation form. The resulting magnetic properties are listed in Table 2 ( $R^{\bullet+}$ ). The computed spin densities are rather different from those observed experimentally. Especially, the HF couplings for the phenoxy ring carbons are inconsistent with the experimentally observed trends. Carbons  $C_3$  and  $C_5$  have HF couplings close to zero; similarly, the analogous couplings for carbons  $C_2$  and  $C_6$  are very small (approx.  $-3.1$  G). The spin density on the phenolic oxygen is significantly smaller (0.137) than the experimentally reported data (see Table 3) and the computed HF coupling for the neighboring phenolic oxygen proton is  $-3.99$  G ( $\rho_H = -0.004$ ).

#### *Tyr radical-His complex*

The geometry of the optimized neutral His-Tyr complex is shown in Fig. 4A together with a representation of the SOMO Kohn-Sham orbital containing the unpaired electron (Fig. 4B). The hydrogen bond distance in the optimized structures of (TRH $^{\bullet}$ ) is 1.90–1.92 Å, in agreement with the majority of the previously reported experimental data (1.81–1.93 Å) [44, 45] and is almost independent on the quality of the double  $\zeta$  basis set used here (1.91, 1.92 and 1.91 Å with 6-31G\*, 6-31+G\* and 6-31++G\*\* basis sets, respectively). In the B3LYP/6-31G\* optimized structure the hydrogen bond makes an angle of 123.7° with the C–O bond of the Tyr radical; the two planes containing the phenoxy and imidazole rings are almost orthogonal and make an angle of 75.8°. For the (TR $^{\bullet-}$ ) the optimized hydrogen bond distance is significantly shorter (1.71, 1.75 and 1.72 Å with 6-31G\*, 6-31+G\* and 6-31++G\*\* basis sets, respectively). The augmentation of the basis set with one or two diffuse functions has only a negligible effect on the optimized hydrogen bond length. The spin distribution on the phenoxy ring in TRH $^{\bullet}$  (see Tables 1 and 2) is slightly different in the optimized Tyr-His complex compared to the isolated Tyr radical. This difference is mainly due to a spin polarization effect through the hydrogen bond formed on complexation with the neighboring His molecule, and varies in

DFT on the magnetic properties of the complex mimicking the  $Y_D^\bullet$  radical in PSII

9

**Table 2.** DFT calculated values of the isotropic part of the hyperfine coupling ( $A_{\text{iso}}$ ) and computed spin density for ring carbons and protons in the model Tyr radical and Tyr-His complex

	C <sub>1</sub>	C <sub>2</sub>	C <sub>3</sub>	C <sub>4</sub>	C <sub>5</sub>	C <sub>6</sub>	$\beta H_1$	$\beta H_2$	H <sub>2</sub>	H <sub>3</sub>	H <sub>5</sub>	H <sub>6</sub>	O <sub>phen</sub>
<b>TR<sup>•</sup></b>													
$\rho$	0.363	-0.133	0.282	-0.070	0.285	-0.134	0.006	0.006	0.006	-0.014	-0.014	0.006	0.409
$A_{\text{iso}}$	12.92	-9.15	7.67	-12.83	7.73	-9.18	5.26	5.27	2.65	-7.01	-6.95	2.62	-9.11
<b>THR<sup>•</sup></b>													
$\rho$	0.371	-0.125	0.266	-0.030	0.269	-0.127	0.005	0.006	0.005	-0.014	-0.013	0.005	0.378
$A_{\text{iso}}$	12.85	-8.76	7.02	-11.12	7.05	-8.82	5.19	6.02	2.44	-6.68	-6.67	2.35	-9.03
<b>TR<sup>•-</sup></b>													
$\rho$	0.355	-0.102	0.224	-0.032	0.254	-0.106	0.001	0.014	0.004	-0.013	-0.012	0.004	0.396
$A_{\text{iso}}$	11.94	-7.41	5.59	-10.89	6.34	-8.06	4.68	9.11	2.02	-6.19	-5.54	1.77	-9.46
<b>THR<sup>•-</sup></b>													
$\rho$	0.248	-0.072	0.162	-0.009	0.163	-0.081	0.003	0.008	0.003	-0.011	-0.010	0.002	0.239
$A_{\text{iso}}$	10.58	-4.83	5.99	-3.99	6.01	-5.14	5.52	6.73	1.33	-3.93	-3.91	1.04	-7.88
<b>THR<sup>•</sup>-1.5 Å</b>													
$\rho$	0.375	-0.121	0.256	-0.004	0.262	-0.121	0.005	0.007	0.005	-0.013	-0.013	0.005	0.355
$A_{\text{iso}}$	12.79	-8.59	6.63	-10.05	6.75	-8.59	5.34	6.17	2.28	-6.56	-6.50	2.23	-8.53
<b>DPTHR<sup>•</sup></b>													
$\rho$	0.346	-0.126	0.276	-0.076	0.263	-0.128	0.008	0.003	0.005	-0.014	-0.013	0.005	0.451
$A_{\text{iso}}$	12.11	-8.77	7.35	-13.19	7.02	-8.46	7.26	2.50	2.55	-6.74	-6.45	2.42	-9.84
<b>TR<sup>•+</sup></b>													
$\rho$	0.317	0.002	0.048	0.206	0.087	0.013	0.001	0.020	-0.002	-0.003	-0.005	-0.001	0.137
$A_{\text{iso}}$	8.82	-3.12	-0.92	2.33	0.06	-3.05	1.80	17.04	-0.85	-1.82	-2.72	-0.84	-5.09

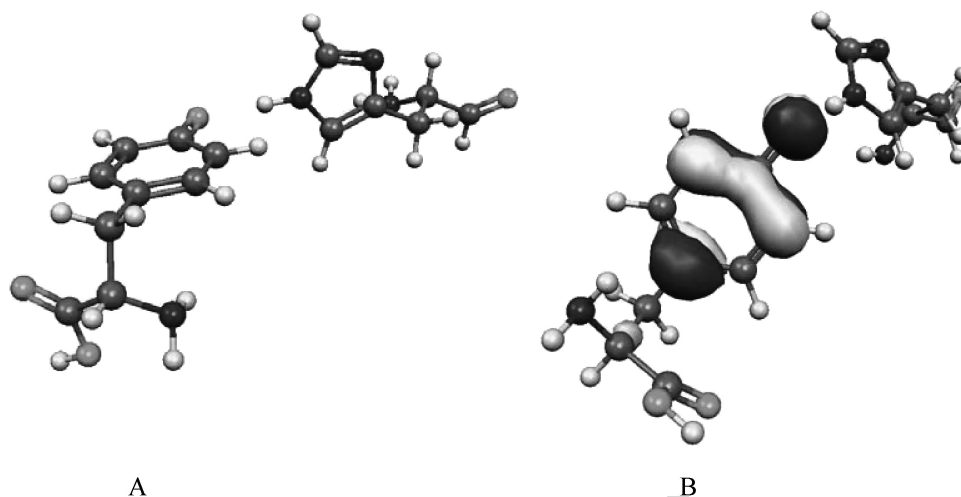


**Figure 4.** (A) DFT optimized structure of the neutral Tyr-His complex radical; (B) Kohn-Sham SOMO orbital containing the unpaired electron for the optimized structure of the neutral Tyr-His complex radical.

magnitude for the different carbons of the phenoxy ring. Comparing this effect between isolated radical and complex, carbons  $C_2$  and  $C_6$  are essentially unaffected ( $\Delta\rho = -0.001$ ,  $\Delta^{13}\text{C } A_{\text{iso}} = -0.2$  G); the same conclusion is made for carbons  $C_3$  and  $C_5$  ( $\Delta\rho = +0.002$ ,  $\Delta^{13}\text{C } A_{\text{iso}} = +0.1$  G). More pronounced changes are observed on the remaining carbons,  $C_1$  and  $C_4$ . An increase in the positive spin density is evident for  $C_1$  ( $\Delta\rho = +0.030$ ,  $\Delta^{13}\text{C } A_{\text{iso}} = +0.8$  G); an analogous effect occurs with the negative spin density on  $C_4$  ( $\Delta\rho = +0.048$ ,  $\Delta^{13}\text{C } A_{\text{iso}} = +2.2$  G), which is the carbon bearing the phenoxy oxygen. The spin-density variations are translated into changes of the hyperfine coupling values for the hydrogen atoms connected to specific carbons. These changes are, as expected, more pronounced for the geometry of the His-Tyr complex with the shortest hydrogen bond length (1.5 Å). The corresponding  $\rho$  and  $^{13}\text{C } A_{\text{iso}}$  values are reported in the bottom section of Table 2 (THR $^\bullet$ ).

The substantial amount of spin present on the phenoxy oxygen is reflected by the calculated spin density on this atom (0.409 for TR $^\bullet$  and 0.378 for THR $^\bullet$ ). It is worthwhile to compare these computational results with the experimentally determined values. By specific  $^{17}\text{O}$ -labeling of the  $Y_D^\bullet$  in PSII, we have determined the spin density for phenolic oxygen to be  $0.28 \pm 0.01$  [46] (this value was previously determined by Warncke [47] and Rigby [48] to be 0.26) for the hydrogen bonded Tyr radical. The spin density for the non-hydrogen bonded Tyr radical in ribonucleotide reductase from *Escherichia coli* was determined by Hoganson *et al.* [49] to be 0.29. This makes a difference in the spin density between H-bonded and non-bonded species of 0.01–0.03 taking into account the experimental uncertainty, which is in agreement with the difference observed in the computed spin densities values (calc.  $\Delta\rho = 0.031$ ). Nevertheless the absolute values of the spin densities

for both, bonded and non-bonded species, are slightly overestimated in our DFT calculations. That could be related to the fact that the spin is strongly polarized between the phenolic oxygen and its nearest neighbor  $C_4$ , which exhibits a negative spin density. Specifically, it is likely that the DFT calculations overestimate the magnitude of this polarization and therefore yield an improperly greater positive spin on the oxygen as well as improperly greater negative spin densities on  $C_4$ . An interesting observation can be made on the relation between the calculated HF coupling for the phenoxy protons and the spin density of the neighboring carbons. Langella *et al.* [19] observed that HF couplings calculated for the hydrogen  $H_3$  and  $H_5$  in various conformers of the Tyr dipeptide analogue follow an almost linear dependence on the  $C_3$  and  $C_5$  spin density. This is not the case, however, for hydrogens  $H_2$  and  $H_6$ , which are believed to interact weakly with the dipeptide backbone. A similar observation is made in our calculation; moreover, the calculated value for the proportionality constant  $Q$  (related to the  $\sigma$ - $\pi$  electron interaction) in the McConnell relation,

$$A_{\text{iso}}(H_\alpha) = Q \cdot \rho_C \quad (4)$$

which describes the relationship between the isotropic hyperfine splitting constant for an  $\alpha$ -proton bound to a planar  $\pi$ -radical, and the unpaired electron spin density  $\rho_C$  at an adjacent  $sp^2$ -hybridized carbon atom, is quite different for the  $H_2$ - $H_6$  and  $H_3$ - $H_5$  pairs. The calculated HF parameters yield average values of  $Q = -19.7$  G for  $H_2$ ,  $H_6$  and  $-24.6$  G for  $H_3$ ,  $H_5$ . This latter value is almost identical with the value of  $-24.9$  G derived from the experimental data for ring protons in various phenoxy compounds [50]. This suggests again that in the estimation of spin density on the Tyr phenoxy ring from the experimental proton coupling constant using the McConnell relation, the use of two slightly different  $Q$  constants for the  $C_2$ ,  $C_6$  and  $C_3$ ,  $C_5$  pairs may be necessary. In order to check if the observed asymmetry is related to the position of the  $\beta$ -hydrogens versus the COOH and  $NH_2$  groups on the Tyr radical backbone, we have also performed the same set of calculations (full relaxation of the geometry) varying the angles between the two  $\beta$  protons and the phenoxy ring for the mirror Tyr enantiomer ( $\gamma_L$  vs.  $\gamma_D$ ). The results show that the same asymmetry is reproduced leading to the same, symmetrically “inverted” curves of the dependence of the  $\beta$ -protons  $A_{\text{iso}}$  on the  $\theta_1$  ( $\theta_2$ ).

It is also worth noting that the calculated results for the model phenoxy radicals (which mimic the Tyr radical) do not show any similar differences for the computed hyperfine couplings of the four phenoxy carbons (and corresponding protons) [12].

Having in mind these “asymmetries” concerning both phenoxy ring protons as well as the  $\beta$ -protons, our computational results can now be compared with the available data from studies of specifically labeled Tyr radicals in the PSII. In general, the calculated spin densities are close to the experimentally determined by various authors (see Table 3). The negative spin density on carbons  $C_2$  and  $C_6$  is nevertheless slightly overestimated by the DFT calculations. The phenolic oxygen

**Table 3.**

Selected experimental values of the  $A_{\text{iso}}$  values and spin densities for ring carbons and protons in various Tyr radicals

	C <sub>1</sub>	C <sub>2</sub>	C <sub>3</sub>	C <sub>4</sub>	C <sub>5</sub>	C <sub>6</sub>	H <sub>2</sub>	H <sub>3</sub>	H <sub>5</sub>	H <sub>6</sub>	O <sub>phen</sub>	Reference
$\rho$	0.38	-0.08	0.25	-0.05	0.25	-0.08					0.29	[49]
	0.32	-0.05	0.21	0.03	0.22	-0.05					0.28	[20]
	0.34	-0.07	0.24	0.02	0.24	-0.07					0.26	[49]
	0.32	-0.04	0.23	0.01	0.23	-0.04					0.26	[22]
	0.37	-0.07	0.24	0.01	0.24	-0.07					0.26	[49]
	0.37	-0.07	0.26	-0.01	0.26	-0.07					0.26	[49]
				-0.03							0.28	[46]
$A_{\text{iso}}$	10.2	-8.3	3.0	-9.7	4.3		1.6	1.6	-6.8	-6.8	-10.5	[20]
	9.3	-8.8	2.7	-9.8	2.7	-8.8	1.6	1.6	-6.4	-6.4	-9.6	[22]
							1.93		-7.03	-6.24		[57]
							2.8	2.8	6.9	6.9		[40]
							1.75	1.75	-6.50	-6.50		[49]
									-6.2	-6.2		[47]
									-6.4	-6.4		[56]

spin density is overestimated as well (*vide supra*), and is calculated in our neutral Tyr-His complex to be 0.387, compared to the values of 0.22 to 0.30 reported in the literature (see Table 3). Nevertheless, it should be mentioned that most values cited in the literature are a sum of the contribution from the phenolic oxygen atom, as well as carbon C<sub>4</sub>; the spin density on this particular carbon cannot be estimated in the same way as on the other phenolic carbons because of the lack of associated proton HF couplings.

An intriguing analogy can be made with recent data reported by Faller *et al.* [45] from a study of possible reaction pathways for the formation of the stable Tyr radical in PSII. In its minimum energy conformation, the DFT calculations on the neutral Tyr radical-imidazole complex reported a hydrogen bond length of 1.93 Å; calculations for the negatively charged diamagnetic Tyr-His pair indicated an optimized distance of 1.52 Å. These findings are in good agreement with our data, which predict 1.90 Å for the neutral Tyr-His complex and 1.61 Å for this same complex in its radical anion form. The important geometrical difference in the optimized structures (the Tyr-imidazole of Faller *et al.* versus our Tyr-His) concerns the mutual orientation of the two rings. In the Faller *et al.* study, the imidazole and phenoxy rings in both optimized geometries remain planar, while our optimization yields the ring-ring angles of 75.8° for the neutral Tyr-His complex and 77.3° for the same complex in its radical-anion form.

Relevant conformational information can also be extracted from the spectroscopic studies of the HF couplings of the imidazole proton in His moiety hydrogen-bonding to the phenolic oxygen of the Tyr radical. It is therefore worth noting that the calculated isotropic part of the HF tensor for this proton in the neutral Tyr-His complex is close to zero (0.13 G), and the dipolar part exhibits moderate values ( $A_{xx} = -1.32$ ,  $A_{yy} = -1.32$ ,  $A_{zz} = 2.64$  G).

*Spin density on the ipso carbon of the Tyr-His model*

As discussed above, most of the studies concerning the spin density distribution over the phenoxy ring in Tyr are based on  $^1\text{H}$ -hyperfine tensors of the phenoxy ring hydrogens and  $^{13}\text{C}$ -hyperfine tensors of specifically labeled ring carbons experimentally determined using CW-EPR spectroscopy. The experimentally reported spin densities are shown in Table 3. It is important to note that the spin densities of the  $\text{C}_4$  ( $\rho_{\text{C}_4}$ , carbon atom connected to the phenoxy oxygen) derived from the CW spectra are very small, in the range of 0.05 to 0.030 [20, 22]. But in the majority of cases the spin density on the carbon  $\text{C}_4$  was estimated as a difference between the overall spin on the phenoxy ring and the sum of the spin density on carbons  $\text{C}_1$ – $\text{C}_3$ ,  $\text{C}_5$  and  $\text{C}_6$ . In order to get an estimate of the related spin density, we have performed additional DFT calculation with focus on the possible hyperfine coupling values for this carbon. The DFT calculated HF tensors elements for the  $\text{C}_4$  carbon in neutral Tyr-His radical (Table 2, THR $^\bullet$ ) are:  $A_{xx} = -19.1$  MHz,  $A_{yy} = -24.7$  MHz,  $A_{zz} = -29.4$  MHz ( $A_{\text{iso}} = -31.1$  MHz) and correspond to the spin density on  $\text{C}_4$  of  $-0.030$ . The HF coupling values are reported in G in Tables 1–3. The corresponding values in MHz are obtained using the conversion factor:  $1 \text{ G} = 2.802 \text{ MHz}$ . This falls in the range of the experimental values previously reported. In order to check how this spin distribution is affected by the mutual orientation of the His molecule and Tyr radical we have performed a scan of its conformational space in order to localize the geometry of the complex for which the calculated  $A_{\text{iso}}$  value is a minimum. The minimum value for the  $\text{C}_4$   $A_{\text{iso}}$  in the whole conformational space is  $-28.3$  MHz and corresponds to a spin density of  $-0.027$ .

 *$^{15}\text{N}$ -ENDOR of the  $\tau$  nitrogen in the His-Tyr complex in PSII*

The ENDOR studies of different hyperfine couplings can be useful as a probe of the local geometry of radicals and molecules. Studies of the selectively labeled nitrogen nuclei were previously performed in our laboratory. The Mims ESE-ENDOR spectra from  $Y_D$   $^{15}\text{N}$ -labeled *Synechocystis* PSII samples exhibit isotropic  $^{15}\text{N}$  hyperfine couplings between the  $Y_D^\bullet$  radical and the D2-His189  $\tau$  nitrogen [51]. Figure 5A is the Mims-ENDOR spectrum of  $Y_D^\bullet$  from globally  $^{15}\text{N}$ -labeled *Synechocystis*. Figure 5B is Mims-ENDOR spectrum of  $Y_D^\bullet$  from *Synechocystis*, where the two His nitrogens have all been isotopically labeled with  $^{15}\text{N}$ . Figure 5C is Mims-ENDOR spectrum of  $Y_D$  from *Synechocystis* where only the  $\pi$  nitrogen of His has been labeled with  $^{15}\text{N}$ . These results show that the isotropic hyperfine coupling is to the  $\tau$  nitrogen, and as a result we inferred that there is a hydrogen bond between  $Y_D^\bullet$  and the His-189  $\tau$  nitrogen [51]. The recently published PSII structure [4] confirms this specific  $Y_D^\bullet$ -H bonding assignment. Additionally, these same spectra show a pair of a broad, dipolar  $^{15}\text{N}$  hyperfine peaks, which were assigned by ENDOR performed on  $Y_D^\bullet$  of PSII  $^{15}\text{N}$  labeled at all Tyr peptide nitrogens, as a dipolar  $^{15}\text{N}$  hyperfine couplings to the peptide nitrogen of Tyr  $Y_D$  (data not

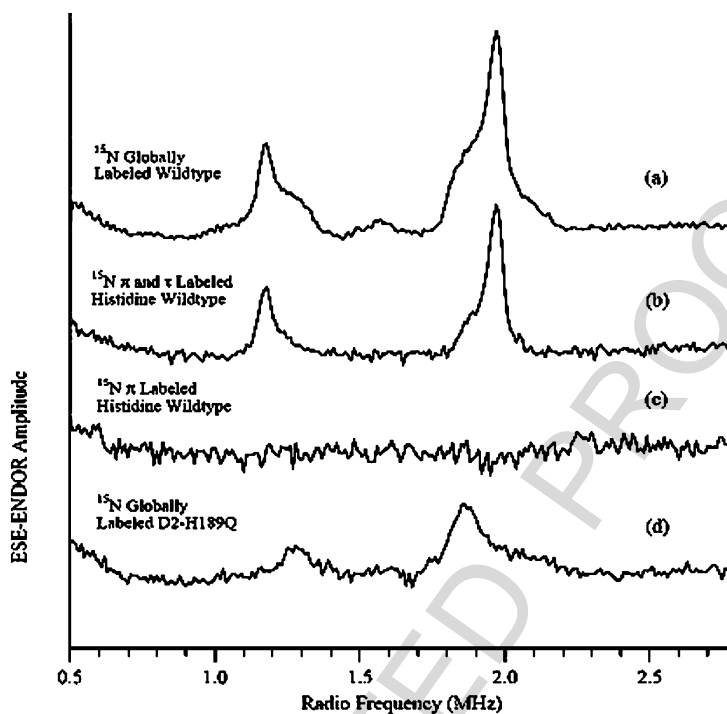


**Figure 5.** Mims ESE-ENDOR spectra of  $Y_D^\bullet$  in *Synechocystis*. (A)  $^{15}\text{N}$  globally labeled wild-type. (B)  $^{15}\text{N}$   $\pi$  and  $\tau$  labeled His wild-type. (C)  $^{15}\text{N}$   $\pi$  labeled His wild-type. (D)  $^{15}\text{N}$  globally labeled D2-H189Q mutant. Adapted from Ref. [51].

shown). To corroborate these results with the DFT predicted magnetic parameters for imidazole ring in His, we have extracted the relevant calculated parameters for  $\pi$  and  $\tau$  nitrogen atoms of His (as well as for the two backbone nitrogens in Tyr and His molecules) from the DFT scan of the conformational space of the Tyr-His complex.

The variation of the  $^{15}\text{N}$   $A_{\text{iso}}$  of the  $\tau$  nitrogen in the His with the changes of the geometry of the Tyr-His complex is plotted in Fig. 6. From Fig. 6A it can be clearly seen that the  $^{15}\text{N}$  coupling decreases with the increase in the hydrogen bond length, following a perfect exponential decay. A very slight variation of the Fermi term (0.05 MHz) is observed when the simultaneous orientation of the planes containing Tyrosine and His ring is varied from coplanarity to the orthogonal conformation (Fig. 6B). The calculated  $^{15}\text{N}$   $A_{\text{iso}}$  of the  $\tau$  nitrogen is most affected by a change in the hydrogen bond angle (ring to ring orientation). For the explanation of the scanned Tyr-His complex geometry see insets in Fig. 6A–D. From Fig. 6C and 6D it can be seen that the maximum  $A_{\text{iso}}$  value is computed when the hydrogen bond angle is close to  $120^\circ$ . This calculated maximum  $^{15}\text{N}$   $A_{\text{iso}}$  value is 2.3 MHz. Another important  $A_{\text{iso}}$  value (1.8 MHz) is found when parallel ring-to-ring orientation is  $120^\circ$ . The calculated value of the hydrogen bond angle in the optimized Tyr-His structure is  $124.3^\circ$  and is smaller than the one proposed by Un

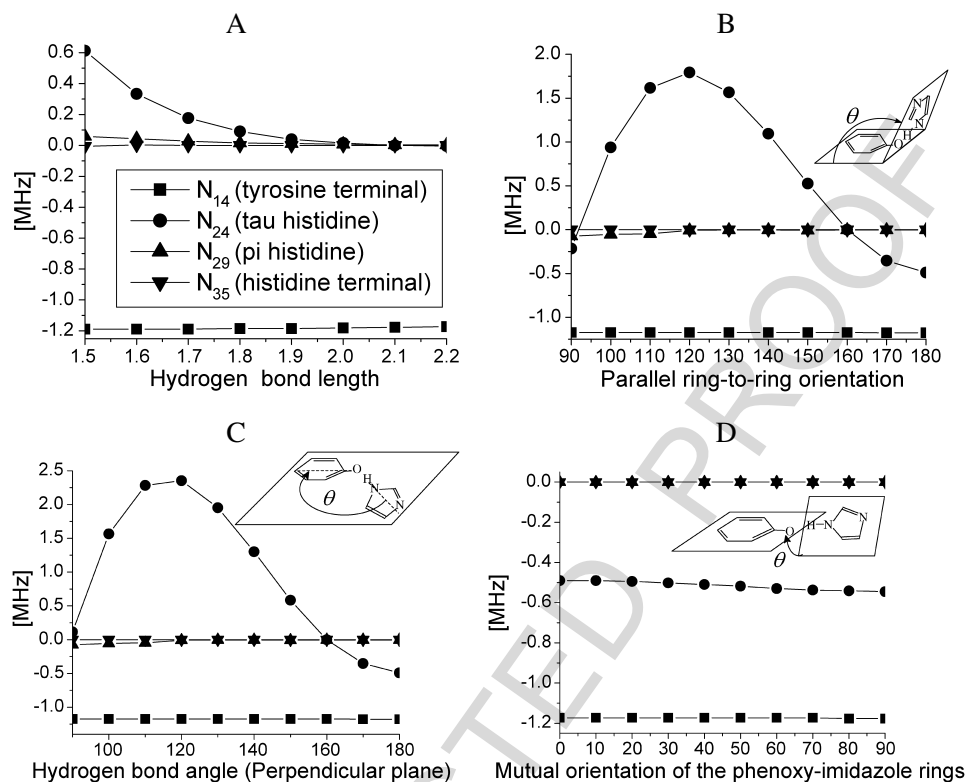


**Figure 6.** DFT calculated values of the  $A_{iso}$  for different nitrogen atoms in the neutral Tyr-His complex radical as a function of the orientation of the His moiety *versus* the Tyr part.  $N_{14}$ , Tyrosine terminal;  $N_{24}$ ,  $\tau$  His;  $N_{29}$ ,  $\pi$  His;  $N_{35}$ , His terminal.  $A_{iso}$  in function of (A) Tyr-phenoxy oxygen-His  $\tau$  hydrogen bond length; (B) parallel Tyr-phenoxy-His imidazole ring to ring orientation; (C) Tyr-phenoxy oxygen-His  $\tau$  hydrogen bond angle; (D) mutual (perpendicular) Tyr-phenoxy-His imidazole ring to ring orientation.

*et al.* (140°) [11] on the basis of the mapping of the MNDO calculated  $g$  values for various conformations of the hydrogen bond to Tyr radical. The experimental 0.09 MHz value corresponds therefore to a structure which could be relatively close to the optimized one for the THR $\bullet$  radical, assuming the hydrogen bond of 1.89 Å.

In the recent  $^{15}\text{N}$  ESE-ENDOR studies on the hydrogen-bonding environment of Tyr radicals in PSII, a non-negligible spin density on the  $\tau$  nitrogen of D2-His189 in  $Y_D^\bullet$  is detected, but no analogous ENDOR signal has been detected from D1-His190 for  $Y_Z^\bullet$  (data not shown). The recently published PSII crystal structure [4] suggests that  $Y_Z^\bullet$  is indeed hydrogen bonded to D1-His190; therefore, one should expect a similar coupling from the  $\tau$  nitrogen of D1-His190. One of the possible reasons, that could explain the lack of similar signal for  $Y_Z^\bullet$ , is that the above mentioned ENDOR study had to be performed on Mn-depleted PSII in order to trap the  $Y_Z^\bullet$  state. Therefore, His interaction could be disrupted as an artifact of the imposed treatment. Nevertheless, in this context it is interesting to note that

for some ring-to-ring orientations of the Tyr-His complex the computed  $A_{\text{iso}}$  values are close to zero. This is for example the case for a hydrogen bond angle close to  $160^\circ$  (see Fig. 6C), which is larger than the value obtained in our optimized Tyr-His structure ( $124.3^\circ$ ) or the one proposed by Un *et al.* ( $140^\circ$ ) [11], but remains within a realistic geometry for the Tyr-His tandem. Thus, another explanation for the lack of the signal from  $\tau$  nitrogen of D1-His190 could be related to a special ring-to-ring orientation of the His to Tyr radical for the  $Y_Z^\bullet$ , which is different from the  $Y_D^\bullet$  form.

The computed  $A_{\text{iso}}$  values for the His  $\pi$  imidazole and backbone nitrogen in our computational model are close to zero. A very small  $A_{\text{iso}}$  of about 0.03 MHz is found on the  $\pi$  nitrogen in His for the shortest hydrogen bond length of 1.5 Å. Another important observation that is straightforward, is that the  $^{15}\text{N}$   $A_{\text{iso}}$  coupling of the Tyr backbone terminal nitrogen is completely insensitive to the changes in the complex geometry. For all different conformations of the complex, this calculated value remains always  $-1.16$  MHz. This is in contrast with our  $^{15}\text{N}$  ENDOR data which indicate a weaker dipolar coupling for the peptide  $Y_D^\bullet$  nitrogen (approx. 0.66 MHz) in *Synechocystis*. Such a difference between the experimental and theoretical values is probably due to the fact that in our computational model, the  $\text{NH}_2$  moiety can gain some additional spin by amino hydrogen-bond coupled spin polarization. The distance between this peptide nitrogen and the carbon  $C_1$  in our optimized structure of the Tyr-His complex is 3.00 Å, which corresponds almost exactly to the distance of 3.01 Å estimated from the  $^{15}\text{N}$  dipolar coupling of 0.09 MHz and  $\rho C_1$  of 0.320 (data not shown).

Bearing in mind this discrepancy and the fact that no computational data are reported for this “peptide” nitrogen, we have decided to carry out an additional set of calculations in which an analogue of dipeptide, similar to that used by Langella *et al.* [19], was used to estimate the hyperfine coupling tensor on the “real” Tyr peptide nitrogen in contrast to our terminal  $\text{NH}_2$  group. To this end an Ala-Tyr-Ala molecule was built and its geometry was fully optimized to one of the local minima and subsequently the EPR parameters were recalculated on this model molecule. The calculated  $^{15}\text{N}$   $A_{\text{iso}}$  coupling on the peptide nitrogen is significantly smaller ( $-0.45$  MHz) than the one calculated on the terminal  $\text{NH}_2$  group in our Tyr-His model ( $-1.16$  MHz) and relatively close to the experimental value of  $Y_D^\bullet$  nitrogen in *Synechocystis* (approx. 0.66 MHz). Interestingly, in the optimized structure of the Ala-Tyr $^\bullet$ -Ala radical, the reorientation of the phenoxy ring versus the backbone peptide chain lead to a configuration (Table 1) in which the orientation of the  $\beta$ -hydrogens ( $\theta_1 = 52.7^\circ$ ,  $\theta_2 = 66.6^\circ$ ) is almost exactly the same as in the one reported experimentally for the Tyr radical in *Synechocystis* sp. PCC 6803 by de Wijn *et al.* [42] ( $\theta_1 = 52 \pm 4^\circ$ ,  $\theta_2 = 68 \pm 4^\circ$ ).

#### *g*-tensor of the Tyr radical and Tyr-His complex

In the early stages of investigation of the Tyr radical in PSII, Un *et al.* presented quantum mechanical calculations of the *g*-tensor dependence on the conformational

geometry of the p-methylphenoxy radical-hydrogen donor [11]. The outlined study was based on Stone's theory for the  $g$  tensor [52, 53] and was performed using semi-empirical MNDO method. Similar DFT calculations were recently presented by Faller *et al.* [45]

Here we calculate the deviation of the  $g$ -tensor elements from the free electron  $g$ -value at different orientation of the His in the Tyr-His complex, in order to understand how the mutual orientation of the hydrogen bond between His and the Tyr radical is translated into changes in the elements of the  $g$  tensor. These results can be easily compared to the experimental data, since multiple high frequency studies have been performed in order to determine the orientation and the shape of the  $g$  tensor in the Tyr radical.

As a first check we have performed a series of computations on the phenoxy radical, the Tyr radical and the Tyr-His complex, in order to determine if the calculated orientation of the  $g$ -tensor *versus* the molecular frame of the Tyr radical is in agreement with the picture proposed almost 40 years ago from a single crystal EPR study of the irradiated HCl-Tyr [54]. For this purpose two independent computational approaches were used; the non-relativistic GIAO as implemented in Gaussian 03, and the GIAO combined with the scalar relativistic Pauli Hamiltonian as implemented in the ADF program. In both approaches, the orientation of the  $g$ -tensor for all of the studied molecules remains constant with respect to the molecular frame of the phenoxy ring: The  $g_{xx}$  axis is oriented along the C–O bond, the  $g_{yy}$  axis lies in the phenoxy ring plane and the  $g_{zz}$  axis is perpendicular to this plane. The presence of the His and its hydrogen bond does not affect this characteristic orientation of the computed  $g$  tensor, as is the case, when a substituent such as for example, thioether group is introduced onto the phenoxy ring [29].

First, analyzing different data from the literature we have noticed that the computed values of the  $g$  tensor elements are in good agreement with those observed in the High-Field EPR studies. From our DFT calculations it is clear that the  $g_{yy}$  and  $g_{zz}$  tensor elements are almost unaffected by the changes in the geometries of the Tyr-His complex (Fig. 7). This is in agreement with other theoretical and experimental studies on the  $g$  tensor in Tyr radical [11, 45, 55]. The calculated values for  $g_{yy}$  (2.0046) and  $g_{zz}$  (2.0022) are almost constant in the whole conformational Tyr-His complex space and are very close to those reported for  $Y_D^\bullet$  in PSII (2.00422 and 2.00211, respectively). The only affected element of the  $g$  tensor is  $g_{xx}$ , the principal axis of which is collinear with the C–O bond of Tyr. This dependency is illustrated in Fig. 7. The strongest dependence is observed with the variation of the hydrogen bond distance. The minimum  $g_{xx}$  value (2.0085) is found for the shortest hydrogen bond length of 1.5 Å, while  $g_{xx} = 2.0101$  is computed at 2.2 Å distance. The mutual orientation of the His imidazole and Tyr phenoxy rings does not substantially affect the  $g_{xx}$  value. For an overall rotation of 90° (from a co-planarity of the His-imidazole and Tyr-phenoxy rings to orthogonal geometry) the computed variation of the  $g_{xx}$  is only  $\Delta g = 0.00016$ . A small decrease in the

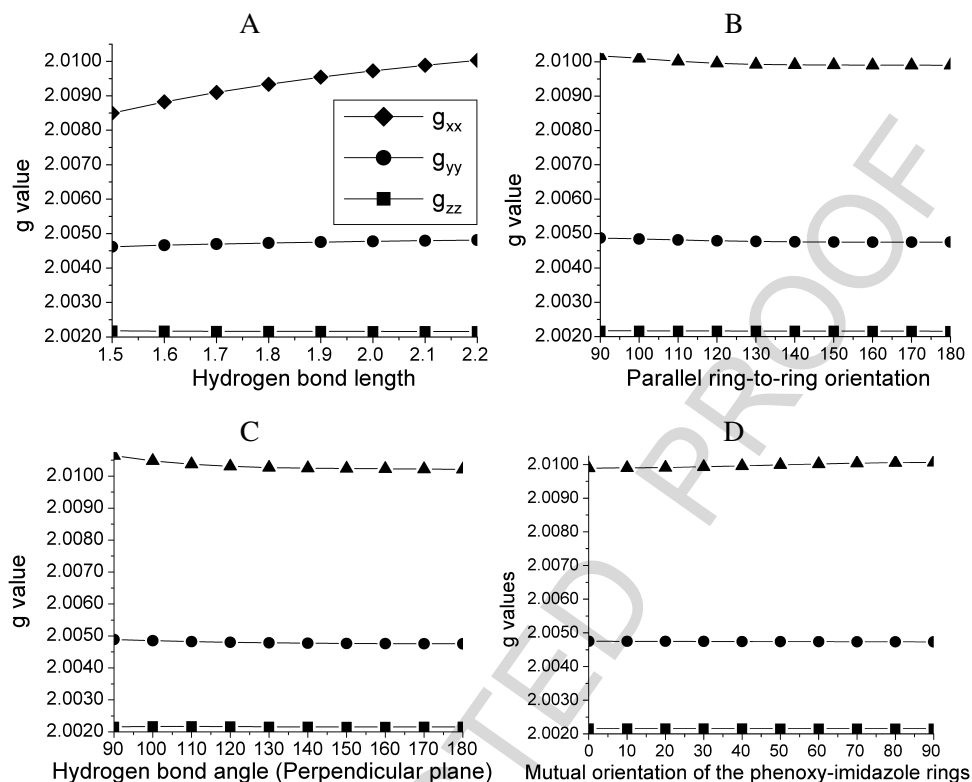


**Figure 7.** DFT calculated values of the  $g$ -tensor elements (GIAO method) for the neutral Tyrosine-His complex radical as a function of the orientation of the His moiety *versus* the Tyr part.  $g$ -tensor elements as function of (A) Tyr-phenoxy oxygen-His  $\tau$  hydrogen bond length; (B) parallel Tyr-phenoxy-His imidazole ring to ring orientation; (C) Tyr-phenoxy oxygen-His  $\tau$  hydrogen bond angle; (D) mutual (perpendicular) Tyr-phenoxy-His imidazole ring to ring orientation.

$g_{xx}$  value (approximately from 2.0106 to 2.0102) is also observed with the variation of the hydrogen bond angle.

The analogous calculations performed on the radical cation form ( $\text{TR}^{\bullet+}$ ) yielded remarkably different  $g$ -tensor values. While  $g_{zz}$  (2.0021) remains close to value calculated for the neutral Tyr-His complex (2.0022), both  $g_{yy}$  (2.0031) and  $g_{xx}$  (2.0044) show significant deviation from the analogous values calculated for  $\text{THR}^{\bullet}$ . This is especially true for the  $g_{xx}$  value, which is clearly out of the experimental range reported for the  $\text{Y}_D^{\bullet}$  radical in PSII (see, for example, Ref. [56]). This result confirms that the protonated radical cation form of the Tyr could be ruled out as a possible intermediate giving rise to the EPR signal in PSII.

## CONCLUSIONS

DFT calculations confirm the differences in the electronic structure and the magnetic properties of the isolated Tyr radical and this same Tyr radical in the neutral

Tyr-His complex. Although small, a net asymmetry is observed in the calculated values of the HF couplings of the two  $\beta$ -protons, as well as in the HF couplings of the protons connected to the phenoxy ring in the Tyr radical. This asymmetry is directly reflected by the different values of the coupling parameter  $B$  (or  $Q$ ) in the McConnell relation estimated from DFT calculations, when considering different protons for both phenoxy protons and the  $\beta$ -hydrogens. Thus, the estimated spin densities can be over (or under) estimated, due to the use of a single  $B$  ( $Q$ ) constant in McConnell relation when analyzing the experimentally determined HF couplings on the Tyr radical.

The DFT predicted hyperfine coupling constant for the  $C_4$  carbon in the Tyr-His model is in accordance with the previously reported values for  $Y_D^\bullet$  in PSII. The spin density calculated for the neighbouring phenoxy oxygen atom is overestimated in our DFT calculations. Presently, we are not able to account for this discrepancy, but suggest that it may be related to the DFT description of this particular system. Further investigations into this possible DFT shortcoming are in progress.

The calculated  $^{15}\text{N}$   $A_{\text{iso}}$  dependence on the geometry of the Tyr-His complex is most pronounced when the hydrogen bond angle (ring-to-ring orientation) is changed, and reproduces quite well the experimental  $^{15}\text{N}$   $A_{\text{iso}}$  value for the tyrosine peptide nitrogen. These  $^{15}\text{N}$   $A_{\text{iso}}$  computations also suggest that for some special Tyr vs. His ring-to-ring orientation, the nitrogen  $A_{\text{iso}}$  vanishes, which is one possible explanation for the recently observed lack of an  $^{15}\text{N}$  ENDOR signal from the  $\tau$  nitrogen of D1-His190 for the Tyr radical  $Y_Z^\bullet$ .

The calculations of the  $g$ -tensor for the Tyr-His complex are in good agreement with the experimental data, but our simplified theoretical model would require a greater level of sophistication in order to reproduce the experimental values for the  $\Delta g$  shift to an acceptable degree of accuracy. For instance, as recently pointed out by Langella *et al.* [19], the inclusion of solvent effects introduced via the continuum solvent model could improve the calculation of magnetic properties. Ultimately, we hope that the results of our DFT calculations on the model Tyr-His complex will be a useful tool for the further interpretation of the experimental EPR properties of Tyr radicals in PSII.

#### *Acknowledgement*

M. B. thanks the Swiss National Science Foundation for the grant for advanced researchers (8220-067593).

#### **REFERENCES**

1. R. J. Debus, *Biochim. Biophys. Acta* **1503**, 164 (2001).
2. B. A. Diner, *Biochim. Biophys. Acta* **1503**, 147 (2001).
3. B. A. Diner and G. T. Babcock, *Adv. Photosynth.* **4**, 213 (1996).
4. K. N. Ferreira, T. M. Iverson, K. Maghlaoui, J. Barber and S. Iwata, *Science* **303**, 1831 (2004).
5. N. Kamiya and J.-R. Shen, *Proc. Natl. Acad. Sci. USA* **100**, 98 (2003).

6. B. Loll, J. Kern, W. Saenger, A. Zouni and J. Biesiadka, *Nature* **438**, 1040 (2005).
7. A. Zouni, H. T. Witt, J. Kern, P. Fromme, N. Krauss, W. Saenger and P. Orth, *Nature* **409**, 739 (2001).
8. P. J. O'Malley and A. J. MacFarlane, *Theochem* **96**, 293 (1992).
9. P. J. O'Malley, A. J. MacFarlane, S. E. J. Rigby and J. H. A. Nugent, *Biochim. Biophys. Acta* **1232**, 175 (1995).
10. Y. Qin and R. A. Wheeler, *J. Am. Chem. Soc.* **117**, 6083 (1995).
11. S. Un, M. Atta, M. Fontecave and A. W. Rutherford, *J. Am. Chem. Soc.* **117**, 10713 (1995).
12. F. Himo, A. Graeslund and L. A. Eriksson, *Biophys. J.* **72**, 1556 (1997).
13. M. J. Lundqvist and L. A. Eriksson, *J. Phys. Chem. B* **104**, 848 (2000).
14. J.-P. Piquemal, J. Maddaluno, B. Silvia and C. Giessen-Prettre, *New J. Chem.* **27**, 909 (2003).
15. M. Engstroem, F. Himo, A. Graeslund, B. Minaev, O. Vahtras and H. Agren, *J. Phys. Chem. A* **104**, 5149 (2000).
16. A. Ivancich, T. A. Mattioli and S. Un, *J. Am. Chem. Soc.* **121**, 5743 (1999).
17. M. Kaupp, T. Gress, R. Reviakine, O. L. Malkina and V. G. Malkin, *J. Phys. Chem. B* **107**, 331 (2003).
18. O. L. Malkina, J. Vaara, B. Schimmelpfennig, M. Munzarova, V. G. Malkin and M. Kaupp, *J. Am. Chem. Soc.* **122**, 9206 (2000).
19. E. Langella, R. Improta and V. Barone, *J. Am. Chem. Soc.* **124**, 11531 (2002).
20. Alia, B. Hulsebosch, H. J. van Gorkom, J. Raap, J. Lugtenburg, J. Matsysik, H. J. M. de Groot and P. Gast, *Chem. Phys.* **294**, 459 (2003).
21. C. T. Farrar, G. J. Gerfen, R. G. Griffin, D. A. Force and R. D. Britt, *J. Phys. Chem. B* **101**, 6634 (1997).
22. R. J. Hulsebosch, J. S. van den Brink, S. A. M. Nieuwenhuis, P. Gast, J. Raap, J. Lugtenburg and A. J. Hoff, *J. Am. Chem. Soc.* **119**, 8685 (1997).
23. I. Ayala, K. Range, D. York and B. A. Barry, *J. Am. Chem. Soc.* **124**, 5496 (2002).
24. P. J. O'Malley, *J. Am. Chem. Soc.* **120**, 11732 (1998).
25. Y.-N. Wang and L. A. Eriksson, *Int. J. Quant. Chem.* **83**, 220 (2001).
26. P. Varnai and W. G. Richards, *Int. J. Quant. Chem.* **84**, 276 (2001).
27. M. R. A. Blomberg, P. E. M. Siegbahn, S. Styring, G. T. Babcock, B. Aakermark and P. Korall, *J. Am. Chem. Soc.* **119**, 8285 (1997).
28. A. M. Boulet, E. D. Walter, D. A. Schwartz, G. J. Gerfen, P. R. Callis and D. J. Singel, *Chem. Phys. Lett.* **331**, 108 (2000).
29. M. Engstrom, F. Himo and H. Agren, *Chem. Phys. Lett.* **319**, 191 (2000).
30. K. E. Wise, J. B. Pate and R. A. Wheeler, *J. Phys. Chem. B* **103**, 4764 (1999).
31. R. G. Evelo, A. J. Hoff, S. A. Dikanov and A. M. Tyryshkin, *Chem. Phys. Lett.* **161**, 479 (1989).
32. W. T. Dixon and D. Murphy, *J. Chem. Soc., Faraday Trans. 2* **72**, 1221 (1976).
33. P. Coppens, Y. Abramov, M. Carducci, B. Korjov, I. Novozhilova, C. Alhambra and M. R. Pressprich, *J. Am. Chem. Soc.* **121**, 2585 (1999).
34. M. J. Frisch, G. W. Trucks, H. B. Schlegel, G. E. Scuseria, M. A. Robb, J. R. Cheeseman, J. A. Montgomery, Jr., T. Vreven, K. N. Kudin, J. C. Burant, J. M. Millam, S. S. Iyengar, J. Tomasi, V. Barone, B. Mennucci, M. Cossi, G. Scalmani, N. Rega, G. A. Petersson, H. Nakatsuji, M. Hada, M. Ehara, K. Toyota, R. Fukuda, J. Hasegawa, M. Ishida, T. Nakajima, Y. Honda, O. Kitao, H. Nakai, M. Klene, X. Li, J. E. Knox, H. P. Hratchian, J. B. Cross, C. Adamo, J. Jaramillo, R. Gomperts, R. E. Stratmann, O. Yazyev, A. J. Austin, R. Cammi, C. Pomelli, J. W. Ochterski, P. Y. Ayala, K. Morokuma, G. A. Voth, P. Salvador, J. J. Dannenberg, V. G. Zakrzewski, S. Dapprich, A. D. Daniels, M. C. Strain, O. Farkas, D. K. Malick, A. D. Rabuck, K. Raghavachari, J. B. Foresman, J. V. Ortiz, Q. Cui, A. G. Baboul, S. Clifford, J. Cioslowski, B. B. Stefanov, G. Liu, A. Liashenko, P. Piskorz, I. Komaromi, R. L. Martin, D. J. Fox, T. Keith, M. A. Al-Laham, C. Y. Peng, A. Nanayakkara, M. Challacombe, P. M. W. Gill, B. Johnson,

- W. Chen, M. W. Wong, C. Gonzalez and J. A. Pople, R. A. *Gaussian 03*. Gaussian, Pittsburgh, PA (2003).
35. P. J. O'Malley, *Chem. Phys. Lett.* **291**, 367 (1998).
  36. J. Gauss, K. Ruud and T. Helgaker, *J. Chem. Phys.* **105**, 2804 (1996).
  37. E. J. Baerends, J. A. Autschbach, A. Bérces, C. Bo, P. M. Boerrigter, L. Cavallo, D. P. Chong, L. Deng, R. M. Dickson, D. E. Ellis, L. Fan, T. H. Fischer, C. Fonseca Guerra, S. J. A. van Gisbergen, J. A. Groeneveld, O. V. Gritsenko, M. Grüning, F. E. Harris, P. van den Hoek, H. Jacobsen, G. van Kessel, F. Kootstra, E. van Lenthe, V. P. Osinga, S. Patchkovskii, P. H. T. Philipsen, D. Post, C. C. Pye, W. Ravenek, P. Ros, P. R. T. Schipper, G. Schreckenbach, J. G. Snijders, M. Sola, M. Swart, D. Swerhone, G. te Velde, P. Vernooijs, L. Versluis, O. Visser, E. van Wezenbeek, G. Wiesenekker, S. K. Wolff, T. K. Woo and T. Ziegler, *ADF2002.03*. Theoretical Chemistry, Vrije Universiteit, Amsterdam (2003). Available online at <http://www.scm.com>
  38. B. A. Barry, M. K. el-Deeb, P. O. Sandusky and G. T. Babcock, *J. Biol. Chem.* **265**, 20139 (1990).
  39. S. A. M. Nieuwenhuis, R. J. Hulsebosch, J. Raap, P. Gast, J. Lugtenburg and A. J. Hoff, *J. Am. Chem. Soc.* **120**, 829 (1998).
  40. D. A. Svistunenko, J. Dunne, M. Fryer, P. Nicholls, B. J. Reeder, M. T. Wilson, M. G. Bigotti, F. Cutruzzola and C. E. Cooper, *Biophys. J.* **83**, 2845 (2002).
  41. C. Tommos, C. Madsen, S. Styring and W. Vermaas, *Biochemistry* **33**, 11805 (1994).
  42. R. de Wijn and H. J. van Gorkom, *Biochim. Biophys. Acta* **1553**, 302 (2002).
  43. R. W. Fessenden and R. H. Schuler, *J. Chem. Phys.* **39**, 2147 (1963).
  44. G. Bar, M. Bennati, H. H. Nguyen, J. Ge, J. A. Stubbe and R. G. Griffin, *J. Am. Chem. Soc.* **123**, 3569 (2001).
  45. P. Faller, C. Goussias, A. W. Rutherford and S. Un, *Proc. Natl. Acad. Sci. USA* **100**, 8732 (2003).
  46. F. Dole, B. A. Diner, C. W. Hoganson, G. T. Babcock and R. D. Britt, *J. Am. Chem. Soc.* **119**, 11540 (1997).
  47. K. Warncke, G. T. Babcock and J. McCracken, *J. Am. Chem. Soc.* **116**, 7332 (1994).
  48. S. E. J. Rigby, J. H. A. Nugent and P. J. O'Malley, *Biochemistry* **33**, 1734 (1994).
  49. C. W. Hoganson, M. Sahlin, B.-M. Sjoeborg and G. T. Babcock, *J. Am. Chem. Soc.* **118**, 4672 (1996).
  50. C. J. Bender, M. Sahlin, G. T. Babcock, B. A. Barry, T. K. Chandrashekar, S. P. Salowe, J. Stubbe, B. Lindstroem, L. Petersson and et al., *J. Am. Chem. Soc.* **111**, 8076 (1989).
  51. K. A. Campbell, J. M. Peloquin, B. A. Diner, X.-S. Tang, D. A. Chisholm and R. D. Britt, *J. Am. Chem. Soc.* **119**, 4787 (1997).
  52. A. J. Stone, *Mol. Phys.* **6**, 509 (1963).
  53. A. J. Stone, *Mol. Phys.* **7**, 311 (1964).
  54. E. L. Fasanello and W. Gordy, *Proc. Natl. Acad. Sci. USA* **62**, 299 (1969).
  55. B. A. Barry and O. Einarsdottir, *J. Phys. Chem. B* **109**, 6972 (2005).
  56. W. Hofbauer, A. Zouni, R. Bittl, J. Kern, P. Orth, F. Lenzian, P. Fromme, H. T. Witt and W. Lubitz, *Proc. Natl. Acad. Sci. USA* **98**, 6623 (2001).
  57. A. Mezzetti, A. L. Maniero, M. Brustolon, G. Giacometti and L. C. Brunel, *J. Phys. Chem. A* **103**, 9636 (1999).